Plasticization-Enhanced Hydrogen Purification Using Polymeric Membranes

Haiqing Lin *et al.*

Science **311**, 639 (2006);
DOI: 10.1126/science.1118079

Science (print ISSN 0036-8075; online ISSN 1095-9203) is published weekly, except the last week in December, by the American Association for the Advancement of Science, 1200 New York Avenue NW, Washington, DC 20005.

electronic spin (*8*–*10*); however, unlike electrons, holes should not have strong hyperfine interactions.

30. We thank S. C. Badescu for helpful discussions. This work was supported by the Defense Advanced Research Projects Agency/Quantum Information Science and Technology, National Security Agency/Army Research Office, U.S. Civilian Research and Development Foundation, Russian Foundation for Basic Research, Russian Science Support Foundation, and Office of Navy Research. E.A.S., I.V.P., M.E.W., and M.F.D. are National Research Council/Naval Research Laboratory Research Associates.

Supporting Online Material

www.sciencemag.org/cgi/content/full/1121189/DC1
Materials and Methods
SOM Text
Table S1
References

11 October 2005; accepted 5 January 2006
Published online 12 January 2006;
10.1126/science.1121189
Include this information when citing this paper.

Plasticization-Enhanced Hydrogen Purification Using Polymeric Membranes

Haiqing Lin,[1,2] Elizabeth Van Wagner,[1] Benny D. Freeman,[1]* Lora G. Toy,[3] Raghubir P. Gupta[3]

Polymer membranes are attractive for molecular-scale separations such as hydrogen purification because of inherently low energy requirements. However, membrane materials with outstanding hydrogen separation performance in feed streams containing high-pressure carbon dioxide and impurities such as hydrogen sulfide and water are not available. We report highly permeable, reverse-selective membrane materials for hydrogen purification, as exemplified by molecularly engineered, highly branched, cross-linked poly(ethylene oxide). In contrast to the performance of conventional materials, we demonstrate that plasticization can be harnessed to improve separation performance.

Hydrogen is produced primarily by steam reforming of hydrocarbons followed by the water-gas shift reaction, which yields a hydrogen product containing impurities such as CO_2, H_2S, and H_2O (*1*). The hydrogen must be purified for further use, and based on the high volumes currently produced and the likelihood for this production to increase, even a small improvement in H_2 purification efficiency could substantially reduce the costs. Membrane technology is attractive for molecular-scale separations because of inherent advantages such as high energy efficiency, excellent reliability, and a small footprint (*2*–*5*). The potential applicability of membrane technology relies strongly on the ability of membrane materials to exhibit high separation performance at practical feed conditions (e.g., with feed streams that contain high-pressure CO_2 and impurities such as H_2S and H_2O).

Highly permeable and highly selective membrane materials are desired for CO_2/H_2 separation. Gas permeability P, which is the steady-state, pressure- and thickness-normalized gas flux through a membrane, is usually expressed as $P = S \times D$, the product of gas solubility S and gas diffusivity D in the polymer membrane (*6*). Selectivity $\alpha_{A/B}$, which characterizes the ability of a membrane to separate gases A and B, is given by

$$\alpha_{A/B} = \frac{P_A}{P_B} = \frac{S_A}{S_B} \times \frac{D_A}{D_B} \qquad (1)$$

where S_A/S_B is the solubility selectivity and D_A/D_B is the diffusivity selectivity (*6*). The selectivity of CO_2 over H_2, α_{CO_2/H_2}, reflects the tradeoff between favorable solubility selectivity (CO_2 is more condensable than H_2 and, therefore, $S_{CO_2}/S_{H_2} > 1$) and unfavorable diffusivity selectivity (CO_2 is larger than H_2, so $D_{CO_2}/D_{H_2} < 1$) (*7*). In conventional polymeric membrane materials (*8*) and those based on carbon (*4*) and silica (*9*, *10*), overall gas selectivity is dominated by diffusivity selectivity and, therefore, these materials are typically more permeable to H_2 than to CO_2. Consequently, the H_2 product is produced in the permeate at low pressure, even though further downstream utilization requires H_2 at high pressure. Expensive recompression of the H_2 product hence diminishes the advantage of membrane technology relative to that of conventional separation technologies, such as pressure swing adsorption, that produce H_2 at or near feed pressure (*1*, *2*, *6*). To minimize or avoid H_2 recompression, optimal membrane materials should be reverse selective (i.e., more permeable to larger molecules, such as CO_2, than to smaller molecules, such as H_2). Here, we propose that to achieve very high CO_2/H_2 selectivity, a membrane must exhibit favorable interactions with CO_2 to enhance solubility selectivity and have very weak size-sieving ability to bring D_{CO_2}/D_{H_2} as close to 1 as possible. Guided by these material design principles, we prepared and characterized a family of highly branched polymers based on poly(ethylene oxide) (PEO) and found that these polymers display excellent CO_2/H_2 separation performance. Counterintuitively, the CO_2/H_2 selectivity and CO_2 permeability improve as CO_2 partial pressure increases (i.e., as CO_2 concentration sorbed in the polymer increases). This is in contrast to the behavior of conventional, strongly size-selective materials, for which raising CO_2 partial pressure typically decreases selectivity (*11*).

In a recent review of the influence of primary chemical structure on CO_2/H_2 separation properties of polymers, ethylene oxide (EO) units were identified as the best chemical groups for such membranes because the polar ether oxygens in EO units interact favorably with CO_2, resulting in high solubility selectivity (*12*). Polymers containing EO can be highly flexible, leading to weak size-sieving behavior and high diffusion coefficients, two factors which contribute directly to high CO_2 permeability and high CO_2/H_2 selectivity (*12*, *13*). However, pure PEO exhibits very low CO_2 permeability [approximately 12 Barrers (*14*) at 35°C and infinite dilution] as a result of high crystallinity levels (*7*). Additionally, the presence of crystalline regions in pure PEO reduces polymer chain mobility in the amorphous phase and increases size-sieving ability, thereby decreasing CO_2/H_2 selectivity (*12*). To circumvent this limitation and effectively frustrate crystallization, short non-PEO segments are introduced into the polymer backbone to interrupt the EO repeat units. Chain branches containing short, noncrystallizable segments of EO are also introduced randomly into the chain backbone to further inhibit crystallinity. This leads to amorphous materials with higher gas permeability and higher CO_2/H_2 selectivity than semicrystalline PEO. Plasticization further improves their CO_2/H_2 separation properties, in contrast to the view that plasticization always reduces polymer membrane separation performance, as it does in the case of CO_2/CH_4 separation in natural gas purification (*15*). Moreover, all polymers are more permeable to CO_2 than to CH_4 because CO_2 has higher diffusivity (because of its smaller molecular size) and higher solubility (because of its greater tendency to condense) than CH_4. In contrast, polymers that are more permeable to CO_2 than to H_2 are much rarer because the smaller size of H_2 favors its permeation over that of the larger CO_2.

[1]Center for Energy and Environmental Resources and Department of Chemical Engineering, University of Texas, Austin, TX 78758, USA. [2]Membrane Technology and Research, 1360 Willow Road, Suite 103, Menlo Park, CA 94025, USA. [3]Center for Energy Technology, Research Triangle Institute, Research Triangle Park, NC 27709, USA.

*To whom correspondence should be addressed. E-mail: freeman@che.utexas.edu

Our family of amorphous, high-molecular-weight, cross-linked, network copolymers was synthesized by photopolymerizing different composition ratios of poly(ethylene glycol) diacrylate [PEGDA: CH_2=CHCOO(CH_2CH_2O)$_{14}$OCCH=CH_2] and poly(ethylene glycol) methyl ether acrylate [PEGMEA: CH_2=CHCO(OCH_2CH_2)$_8$$OCH_3$] (*16*, *17*). The resulting copolymer network has the general chemical structure shown in Fig. 1. PEGDA contains EO units in its backbone, and PEGMEA has pendant EO units. Cross-linked copolymer samples with 0 to 99 weight percent (wt %) PEGMEA and the balance PEGDA were prepared and characterized. Independent of the concentration of PEGDA and PEGMEA, the copolymers contain about 82 wt % EO. Increasing PEGMEA content increases fractional free volume and, in turn, CO_2 permeability and pure-gas CO_2/H_2 selectivity. However, at low temperatures (≤0°C), materials with very high PEGMEA content (e.g., 91 wt %) crystallize, resulting in a substantial permeability decrease below 0°C. We extensively investigated the CO_2/H_2 permeation properties of the 70 wt % PEGMEA/30 wt % PEGDA copolymer at –20°, 10°, and 35°C with pure gases and three binary CO_2/H_2 mixtures of different compositions (*16*). We chose this temperature range not only because this copolymer does not crystallize over this range but also because this range is consistent with the operating temperature of some industrial processes currently used for H_2 purification (*1*). Additionally, to determine the effect of H_2O and H_2S impurities on CO_2/H_2 separation properties, the 91 wt % PEGMEA/9 wt % PEGDA copolymer was characterized at 22°C with a moisture-laden CO_2/H_2 mixture and a four-component, H_2S-containing gas mixture that mimicked the composition of process synthesis gas. In both pure- and mixed-gas studies, the PEGMEA/PEGDA films were physically stable at transmembrane pressure differences up to 21 atm (the maximum value explored in our study), and their gas permeability coefficients were independent of previous thermal and gas exposure history, as expected for rubbery polymers. Permeability coefficients were independent of film thickness, which varied from 70 to 500 μm.

Figure 2 shows the dependence of CO_2 and H_2 permeability coefficients on CO_2 partial pressure in the feed at different temperatures. As CO_2 partial pressure increases, CO_2 and H_2 permeabilities increase at all temperatures; the permeability rise is greater at lower temperatures because of higher CO_2 thermodynamic activity (at a fixed partial pressure) in the polymer film at cooler temperatures. Both pure- and mixed-gas permeabilities also follow the same trends, suggesting that the permeability increase is in large measure a result of increasing CO_2 partial pressure. As indicated by an increase in CO_2 diffusivity with increasing CO_2 concentration in the film (*18*), CO_2 sorbed in the polymer plasticizes the polymer chains, leading to an increase in fractional free volume and, in turn, gas permeability. With decreasing temperature, CO_2 sorption and, hence, plasticization increase so that the effect of CO_2 partial pressure on permeability becomes even stronger.

Decreasing temperature typically decreases gas permeability as a result of a reduction in polymer chain mobility and, therefore, diffusivity at lower temperatures (*6*, *19*). However, Fig. 2A demonstrates that decreasing temperature does not necessarily decrease CO_2 permeability, especially at high CO_2 partial pressure. For example, at a CO_2 feed partial pressure of 17 atm, the CO_2 permeability at –20°C is 410 Barrers, which is higher than that at 10°C (300 Barrers) and very similar to that at 35°C (440 Barrers). Thus, the permeability decrease that would normally accompany a temperature reduction is essentially offset by the increase in CO_2 solubility and the increased plasticization of the polymer by CO_2, which increases diffusivity at lower temperatures.

Decreasing temperature considerably increases mixed-gas CO_2/H_2 selectivity. As shown in Fig. 3, at a CO_2 partial pressure of 17 atm, mixed-gas selectivity increases from 9.4 to 31 as temperature decreases from 35° to –20°C. Furthermore, the selectivity of 31 is accompanied by a CO_2 permeability of 410 Barrers, which is orders of magnitude higher than that observed in conventional polymer membranes used for CO_2 separations (*6*). Facilitated transport membranes can exhibit high CO_2/light gas selectivity at low CO_2 partial pressure (~1 atm or less); however, the selectivity in these materials decreases strongly as CO_2 pressure increases (*20*–*22*). Such materials are often studied for low CO_2 partial pressure applications (e.g., removal of CO_2

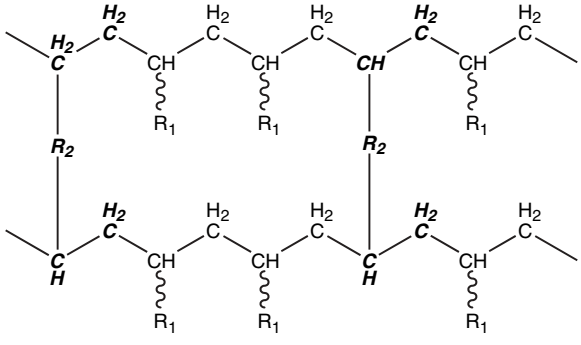

Fig. 1. Schematic representation of PEGDA/PEGMEA copolymer network. Italicized and bolded parts of the network derive from the cross-linker. R_1 is CO(OCH_2CH_2)$_8$$OCH_3$ from PEGMEA; R_2 is COO(CH_2CH_2O)$_{14}$OC from PEGDA.

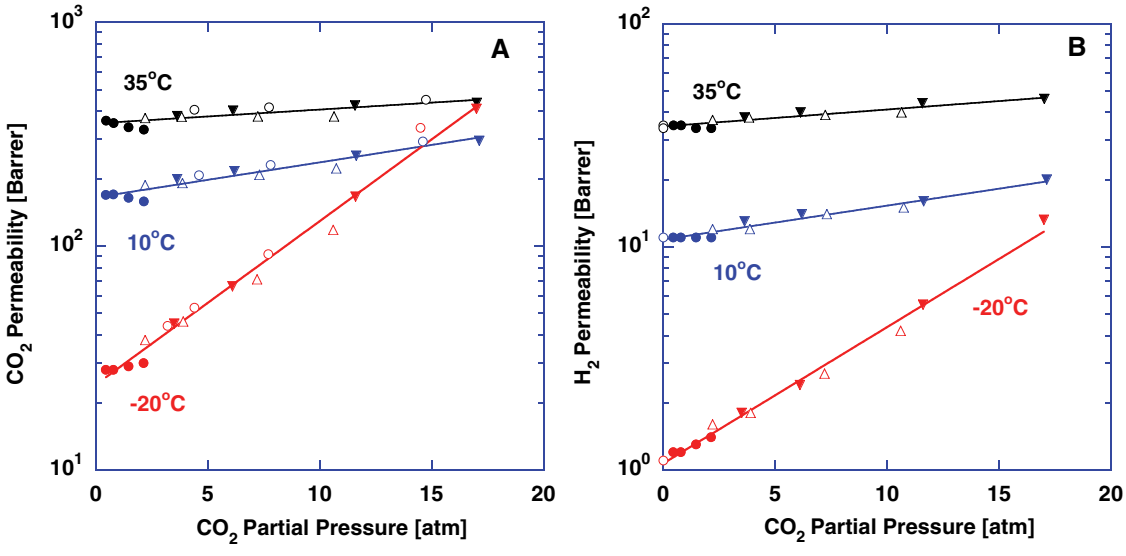

Fig. 2. Effect of temperature and CO_2 upstream partial pressure on (**A**) pure- and mixed-gas CO_2 permeability and (**B**) pure- and mixed-gas H_2 permeability in 70 wt % PEGMEA/30 wt % PEGDA copolymer (*14*). Pure-gas permeability data are shown as open circles (○). Mixed-gas CO_2/H_2 feed compositions (in mol % CO_2:mol % H_2) were 10:90 (●), 50:50 (Δ), and 80:20 (▼). Uncertainty in the permeability data was ±10% or less. The lines are provided to guide the eye.

from breathing gas aboard spaceships (*20*). However, they cannot operate at the high pressures required for hydrogen applications because they are often based on liquids supported in porous media, and the liquids typically cannot be maintained in the porous support when a large pressure difference is applied across the membrane (*23*, *24*).

Mixed-gas selectivity is essentially independent of CO_2 partial pressure at 35° and 10°C (Fig. 3). However, as CO_2 partial pressure increases at –20°C, mixed-gas CO_2/H_2 selectivity increases by 35%. In conventional size-sieving polymers, plasticization of the polymer by CO_2 or other condensable components results in mixed-gas selectivity values that decrease, often markedly, as CO_2 partial pressure increases (*11*) or when other strongly sorbing impurities such as higher hydrocarbons are present (*25*). For example, when the CO_2 partial pressure increased from 1 to 10 atm, the CO_2/CH_4 selectivity of a rigid, glassy, strongly size-sieving, aromatic polyimide decreased from 40 to about 4 (*11*).

We ascribe the mixed-gas CO_2/H_2 selectivity results for the PEGMEA/PEGDA copolymers to the inherent transport properties of these reverse-selective materials (*3*, *26*). At high CO_2 partial pressures, these materials sorb considerable amounts of CO_2, leading to swelling and an increase in free volume, which presumably decreases the glass transition temperature (T_g) (*27*–*29*) and weakens the size-sieving ability of the membrane (*26*).

Figure 4 presents a permeability/selectivity map for CO_2/H_2 separation. The upper bound line in the figure gives an estimate of the highest pure-gas selectivity possible for a given permeability in polymer-based materials at 25°C (*8*). Unlike separation based on strong size-sieving ability [where there is a strong tradeoff between permeability and selectivity (*8*, *30*)], the positive slope of the upper bound indicates that high CO_2 permeability and high CO_2/H_2 selectivity may be achieved simultaneously. The PEGMEA/PEGDA copolymers we explored exhibit excellent separation performance for CO_2/H_2 mixtures, and decreasing temperature actually moves the CO_2/H_2 separation performance above the upper bound line. However, because this line is commonly established by permeation properties of polymers at or near 25°C (*8*), the upper bound may shift as temperature deviates from 25°C. Currently, there is no model to predict the temperature dependence of the upper bound, and there are not yet enough systematic experimental data available to provide clear evidence of its temperature dependence.

The effect of impurities such as H_2O and H_2S on CO_2/H_2 separation properties was investigated at 22°C with the 91 wt % PEGMEA/9 wt % PEGDA copolymer. Although this material crystallizes at about 0°C, it is wholly amorphous at the experimental temperature studied. Because it contains more PEGMEA, this copolymer is more permeable than the 70 wt % PEGMEA/30 wt % PEGDA material presented in Figs. 2 to 4. At 25°C, the infinite-dilution CO_2 permeability is 380 Barrers for the 91 wt % PEGMEA copolymer and 280 Barrers for the 70 wt % PEGMEA material. The addition of 0.33 mole percent (mol %) H_2O vapor (i.e., 100% relative humidity) to a feed gas containing a 1:3 mixture of CO_2:H_2 at 22°C and a feed pressure of 8.0 atm increased CO_2 permeability of the 91 wt % PEGMEA copolymer from 360 to 515 Barrers and its mixed-gas CO_2/H_2 selectivity from 7.8 to 12. We ascribe this change to plasticization by H_2O, which tends to improve CO_2/H_2 separation performance by a mechanism probably very similar to that by which higher CO_2 partial pressure increases CO_2/H_2 selectivity.

The 91 wt % PEGMEA copolymer was also evaluated with a four-component gas mixture composition representative (on a dry basis) of a synthesis gas stream produced by a commercial General Electric (formerly, Texaco) quench gasifier (*31*). This mixture contained 1.0% H_2S, 12.5% CO_2, and 35.7% H_2 in CO. The separation of H_2S from H_2, similar to that of CO_2 from H_2, requires reverse-selective membrane materials with weak size-sieving ability and a polar nature to interact more favorably with this acid gas. At a feed pressure of 7.8 atm, the copolymer had an H_2S permeability of 2500 Barrers and a mixed-gas H_2S/H_2 selectivity of 50. H_2S is considerably more soluble than CO_2 in polar polymers (*32*, *33*), and this effect contributes to the much higher H_2S permeability than CO_2 permeability in the material. Additionally, CO_2 permeability and CO_2/H_2 selectivity remain unchanged in the presence of H_2S, indicating the robustness of this series of polymers for CO_2/H_2

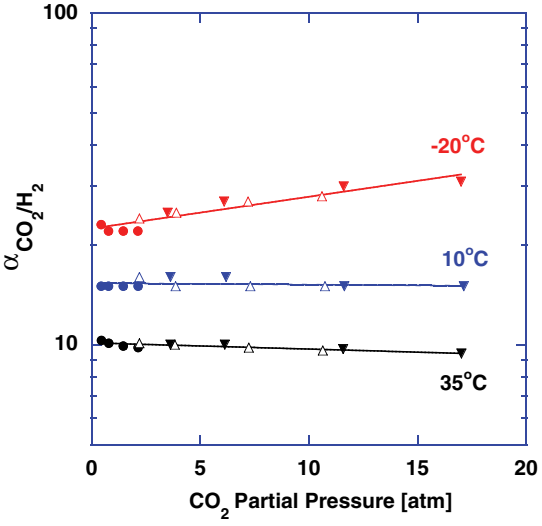

Fig. 3. Effect of CO_2 partial pressure and temperature on mixed-gas CO_2/H_2 selectivity (α_{CO_2/H_2}) in 70 wt % PEGMEA/30 wt % PEGDA copolymer. Mixed-gas CO_2/H_2 feed compositions (in mol % CO_2:mol % H_2) were 10:90 (●), 50:50 (Δ), and 80:20 (▼). The lines are provided to guide the eye.

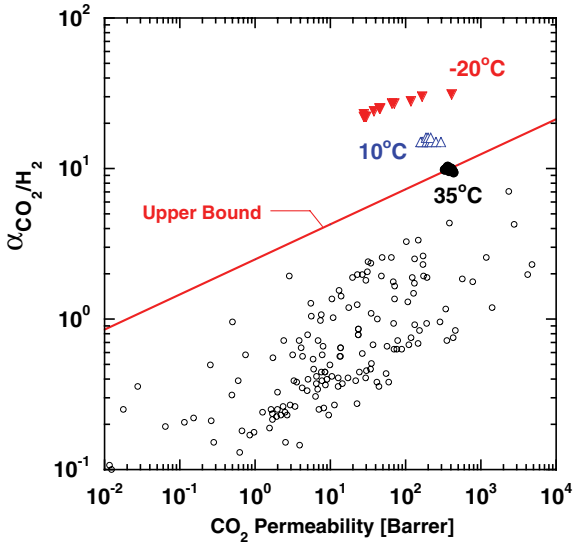

Fig. 4. Permeability/selectivity map for CO_2/H_2 separation. Mixed-gas separation performance data of the 70 wt % PEGMEA/30 wt % PEGDA copolymer at 35°C (●), 10°C (Δ) and –20°C (▼) are included for comparison. The various symbols at each temperature represent data points measured at different feed pressures and binary CO_2/H_2 mixture compositions. Each open circle on the graph represents the separation characteristics of a different material from the literature. Data at lower CO_2 permeability correspond to lower CO_2 partial pressures in the feed gas and vice versa. The upper bound is drawn according to a model prediction of this phenomenon (*30*) with the adjustable parameter f set to 0. The parameter f characterizes the interchain spacing at equilibrium. Rubbery polymers such as those of interest in this work do not exhibit the nonequilibrium excess volume that is associated with nonzero values of f in glassy polymers.

separation. If the H_2S partial pressure were higher, it might sorb to high enough levels to alter the gas transport properties of the polymer.

In summary, a family of reverse-selective membrane materials based on highly branched, cross-linked PEO exhibits outstanding separation performance for H_2 purification by removing acid gases such as CO_2 and H_2S from feed streams of practical interest. Moreover, the presence of moisture and high-pressure CO_2 in the feed actually improves permeability and selectivity, in contrast to the detrimental behavior associated with plasticizing agents in conventional membrane materials. In addition to hydrogen purification applications, these molecularly engineered copolymers may also be used to remove CO_2 and H_2S from natural gas as well as SO_2 and NH_3 from nonpolar gases.

References and Notes

1. A. L. Kohl, R. B. Nielsen, *Gas Purification* (Gulf Publishing, Houston, TX, ed. 5, 1997).
2. J. M. S. Henis, M. K. Tripodi, *Science* **220**, 11 (1983).
3. T. C. Merkel *et al.*, *Science* **296**, 519 (2002).
4. M. B. Shiflett, H. C. Foley, *Science* **285**, 1902 (1999).
5. Z. Lai *et al.*, *Science* **300**, 456 (2003).
6. R. W. Baker, *Membrane Technology and Applications* (Wiley, New York, ed. 2, 2004).
7. H. Lin, B. D. Freeman, *J. Membr. Sci.* **239**, 105 (2004).
8. L. M. Robeson, *J. Membr. Sci.* **62**, 165 (1991).
9. R. M. de Vos, H. Verweij, *Science* **279**, 1710 (1998).
10. A. Yamaguchi *et al.*, *Nat. Mater.* **3**, 337 (2004).
11. C. Staudt-Bickel, W. J. Koros, *J. Membr. Sci.* **155**, 145 (1999).
12. H. Lin, B. D. Freeman, *J. Mol. Struct.* **739**, 57 (2005).
13. I. Blume, I. Pinnau, U.S. Patent 4, 963, 165 (1990).
14. 1 Barrer $= 10^{-10} \frac{cm^3\ (STP)\ cm}{cm^2\ s\ cm\ Hg}$, where STP is standard temperature and pressure.
15. A. Bos, I. Punt, H. Strathmann, M. Wessling, *Am. Inst. Chem. Eng. J.* **47**, 1088 (2001).
16. Materials and methods are available as supporting material on *Science* Online.
17. H. Lin, T. Kai, B. D. Freeman, S. Kalakkunnath, D. S. Kalika, *Macromolecules* **38**, 8381 (2005).
18. H. Lin, B. D. Freeman, in preparation.
19. R. M. Barrer, *Nature* **140**, 106 (1937).
20. H. Chen, A. S. Kovvali, K. K. Sirkar, *Ind. Eng. Chem. Res.* **39**, 2447 (2000).
21. R. Quinn, D. V. Laciak, *J. Membr. Sci.* **131**, 49 (1997).
22. M. Teramoto, S. Kitada, N. Ohnishi, H. Matsuyama, N. Matsumiya, *J. Membr. Sci.* **234**, 83 (2004).
23. A. S. Kovvali, H. Chen, K. K. Sirkar, *J. Am. Chem. Soc.* **122**, 7594 (2000).
24. E. L. Cussler, in *Polymeric Gas Separation Membranes*, D. R. Paul, Y. P. Yampol'skii, Eds. (CRC Press, Boca Raton, FL, 1994), pp. 273–300.
25. L. S. White, T. A. Blinka, H. A. Kloczewski, I.-F. Wang, *J. Membr. Sci.* **103**, 73 (1995).
26. I. Pinnau, Z. He, *J. Membr. Sci.* **244**, 227 (2004).
27. T. S. Chow, *Macromolecules* **13**, 362 (1980).
28. J. S. Chiou, J. W. Barlow, D. R. Paul, *J. Appl. Polym. Sci.* **30**, 2633 (1985).
29. A. F. Ismail, W. Lorna, *Sep. Purif. Technol.* **27**, 173 (2002).
30. B. D. Freeman, *Macromolecules* **32**, 375 (1999).
31. R. P. Gupta, K. C. O'Brien, *Ind. Eng. Chem. Res.* **39**, 610 (2000).
32. W. Heilman, V. Tammela, J. A. Meyer, V. Stannett, M. Szwarc, *Ind. Eng. Chem.* **48**, 821 (1956).
33. P. Y. Hsieh, *J. Appl. Polym. Sci.* **7**, 1743 (1963).

34. We gratefully acknowledge partial support of this work by the U.S. Department of Energy (grant no. DE-FG03-02ER15362) and NSF (grant no. CTS-0515425). This research was also partially supported by the U.S. Department of Energy's National Energy Technology Laboratory under subcontract from Research Triangle Institute through the prime contract no. DE-AC26-99FT40675.

Supporting Online Material

www.sciencemag.org/cgi/content/full/311/5761/639/DC1
Materials and Methods
References

28 July 2005; accepted 20 December 2005
10.1126/science.1118079

Asymmetric Hydrogenation of Unfunctionalized, Purely Alkyl-Substituted Olefins

Sharon Bell,[1]* Bettina Wüstenberg,[1]* Stefan Kaiser,[1] Frederik Menges,[1] Thomas Netscher,[2] Andreas Pfaltz[1]†

Asymmetric hydrogenation of olefins is one of the most useful reactions for the synthesis of optically active compounds, especially in industry. However, the application range of the catalysts developed so far is limited to alkenes with a coordinating functional group or an aryl substituent next to the double bond. We have found a class of chiral iridium catalysts that give high enantioselectivity in the hydrogenation of unfunctionalized, trialkyl-substituted olefins. Because these catalysts do not require the presence of any particular functional group or aryl substituent in the substrate, they considerably broaden the scope of asymmetric hydrogenation.

Asymmetric hydrogenation is one of the most widely used, most reliable catalytic methods for the preparation of optically active compounds (*1*–*3*). High enantioselectivity, low catalyst loadings, essentially quantitative yields, and mild conditions are attractive features of this transformation. Since the early 1970s, when the well-known L-DOPA (L-dioxyphenylalanine) process was established at Monsanto (*3*), hydrogenation has played a dominant role in industrial asymmetric catalysis (*4*). An enormous variety of chiral phosphine ligands has been developed, many of which induce very high enantioselectivity in rhodium- and ruthenium-catalyzed hydrogenations.

However, despite great progress during recent decades, the range of olefins that can be hydrogenated with high enantiomeric excess (ee) is still limited. Both rhodium and ruthenium catalysts require the presence of a polar functional group next to the C=C bond, which can coordinate to the metal center. Hydrogenation of dehydro–amino acid derivatives or allylic alcohols are typical examples. With unfunctionalized olefins, these catalysts generally show low reactivity and unsatisfactory enantioselectivity. Therefore, their application is restricted to certain classes of properly functionalized substrates.

Some years ago, we introduced iridium complexes with chiral P,N ligands (ligands with coordinating P and N atoms) as catalysts that overcome these limitations (Fig. 1) (*5*–*19*). Various unfunctionalized aryl-substituted olefins can be hydrogenated with high enantioselectivity and high catalytic efficiency using catalysts of this type. Nonetheless, satisfactory

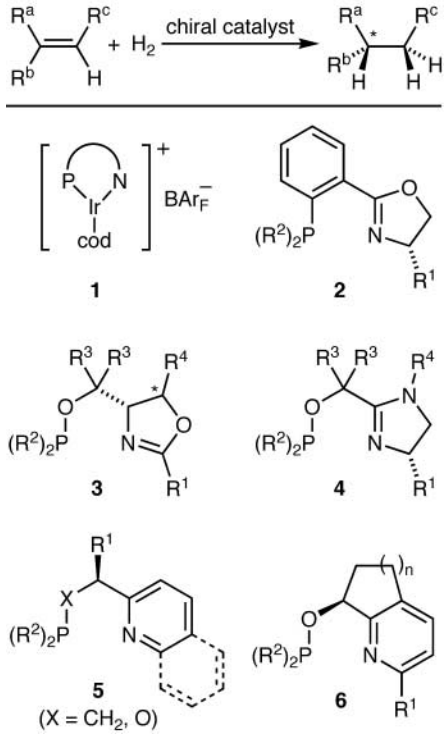

Fig. 1. Asymmetric hydrogenation of olefins with iridium catalysts **1** derived from chiral ligands **2** to **6**. Abbreviations: cod, cycloocta-1,5-diene; BAr_F, tetrakis[bis-3,5-(trifluoromethyl)phenyl]borate.

[1]Department of Chemistry, University of Basel, St. Johanns-Ring 19, CH-4056 Basel, Switzerland. [2]Research and Development, DSM Nutritional Products Ltd., P.O. Box 3255, CH-4002 Basel, Switzerland.

*These authors contributed equally to this work.
†To whom correspondence should be addressed. E-mail: andreas.pfaltz@unibas.ch